

# Rapid separation of L-gossypol using chiral derivatizing reagent combined with ultrasonic crystallization

Yun Zhou<sup>a,b,†</sup>, Yizhuo Li<sup>a,†</sup>, Ke Li<sup>b</sup>, Junfeng Zhang<sup>b</sup>, Xueping Li<sup>b,\*</sup>, Daocheng Wu<sup>c,\*</sup>

<sup>a</sup> College of Clinical Medicine, Xi'an Medical University, Xi'an 710021 China

<sup>b</sup> Xi'an Key Laboratory for Prevention and Treatment of Common Aging Diseases, Translational and Research Centre for Prevention and Therapy of Chronic Disease, Institute of Basic and Translational Medicine, Xi'an Medical University, Xi'an 710021 China

<sup>c</sup> Key Laboratory of Biomedical Information, Engineering of Education Ministry, School of Life Science and Technology, Xi'an Jiaotong University, Xi'an 710049 China

\*Corresponding authors, e-mail: wudaocheng@mail.xjtu.edu.cn, lxp\_lucy@qq.com

† These authors contributed equally to this work.

Received 20 Feb 2024, Accepted 28 Jun 2025  
Available online

**ABSTRACT:** Gossypol, a natural polyphenolic compound, has notable medicinal and economic value due to its strong antitumor activity. Its primary active form, levorotatory gossypol (L-gossypol), exhibits optical activity. However, the existing methods for separating L-gossypol face challenges such as complexity, low yield, and high costs. Traditional techniques like column chromatography are unsuitable for industrial-scale production. While the crystallization separation could achieve gram-scale yields with relatively lower overall costs, ensuring purity required several days for one production cycle. In this study, we innovatively employed a combination of a chiral derivatizing reagent (CDR) and ultrasonic crystallization to achieve a rapid and cost-effective separation of L-gossypol. Ultrasonic crystallization uses ultrasound-induced cavitation to drive crystallization. The method involves the use of an economical chiral resolving agent, specifically (S)-1-(p-nitrophenyl)-1,3-dihydroxypropanamine, which reacts with racemic gossypol to produce derivatives with distinct physical properties. Ultrasonic crystallization in ethyl acetate serves to efficiently crystallize L-gossypol derivatives. Acid hydrolysis is then employed to remove the chiral resolving agent, resulting in high-purity L-gossypol products. Notably, this streamlined process reduces the separation duration from 4 days, as reported in existing literature, to a single day. Establishing a cyclic process enables continuous production of substantial amounts of high-purity L-gossypol. Within 24 h, crystal yield reached 43.80% with 97.89% optical purity; after hydrolysis, the total yield was 40.45% with 97.07% optical purity. Furthermore, the separated L-gossypol samples exhibit significant antitumor activity. The developed approach offers a promising application prospect for enhancing the efficiency and scalability of L-gossypol production in industrial settings.

**KEYWORDS:** gossypol, chiral resolution, L-gossypol, ultrasonic crystallization, threo(-)-1-(p-nitrophenyl)-1,3-dihydroxypropylamine

## INTRODUCTION

Gossypol, characterized as a polyphenolic hydroxyl binaphthalene compound, presents itself as a yellow-colored solid substance with limited aqueous solubility. Its chemical structure is identified as (2,2'-binaphthalene)-8, 8'-dicarboxaldehyde, 1, 1', 6, 6', 7, 7'-hexahydroxy-5, 5'-diisopropyl-3, 3'-dimethyl [1]. Predominantly found in various organs of cotton sunflower plants, particularly in cottonseed, gossypol boasts a broad spectrum of biological activities. These encompass antifertility, antimalarial, antitumor, antibacterial, antidiabetic, and antiviral properties. Especially in the field of antitumor therapy, it has shown notable potential, significantly contributing to its economic value. [2–7].

Despite lacking a chiral atom, gossypol exhibits optical activity due to the C-C single bond linking the 2 naphthalene planes, restricting free rotation. In its natural state, gossypol typically exists as 2 optical isomers: L-gossypol [(+)-gossypol] and D-gossypol [(-)-gossypol] [8]. A study investigating the cytotox-

icity of L-, D-, and racemic gossypol on HeLa cells revealed that D-gossypol lacks cytotoxicity, whereas L- and racemic gossypol inhibit cell synthesis, division, and proliferation. The racemic gossypol demonstrates only a fraction of the effectiveness against tumor cells compared to L-gossypol, indicating that the active component in racemic gossypol is likely L-gossypol [9].

Racemate resolution stands out as an effective approach for obtaining pure enantiomers, with various chiral resolution methods in current use. These methods encompass crystallization resolution, inclusion resolution, digestion resolution, molecular imprinting, TLC chromatography, gas chromatography, high-performance liquid chromatography, high-performance supercritical fluid chromatography, and high-performance capillary electrophoresis [10]. Historically, the preparation of L-gossypol predominantly relied on column chromatography [11]. Some research teams have explored direct chiral gossypol extraction through crystallization, resulting in the formation of single crystals of gossypol enantiomers [12]. However, these methods face several limitations that

pose significant challenges in advancing large-scale production, including complexity, time consumption, high costs, and low yields. Additionally, the biological activity of L-gossypol obtained through these methods remains unverified. Hence, there is a critical need to develop a simple and efficient method for the rapid preparation of L-gossypol that can be readily scaled up.

To solve this problem, we have carefully investigated the characteristics of various existing L-gossypol separation methods and determined a new separation strategy based on actual needs. This study aims to tackle the challenges associated with the separation of L-gossypol by introducing a novel and efficient technique that utilizes chiral resolving agents and ultrasound-enhanced crystallization. Fig. 1 shows the process: the resolving agent threo(-)-1-(p-nitrophenyl)-1,3-dihydroxypropylamine forms L-gossypol derivatives and seed crystals. These are added to a derivative solution, where ultrasonic crystallization enables continuous purification. Acid hydrolysis then removes the resolving agent, yielding high-purity L-gossypol. From a mechanistic standpoint, ultrasound crystallization technology capitalizes on the cavitation effect of ultrasound to shift the crystallization-dissolution equilibrium towards crystallization. Ultrasound facilitates nucleation by reducing supersaturation, enhancing product quality, shortening crystallization time, and improving efficiency. This simplifies separation steps and increases product yield [13]. In comparison with the improved column chromatography for L-gossypol preparation, the ultrasonic-induced crystallization method further streamlines resolution steps, reduces crystallization time, and lowers preparation costs. While previous methods required over 4 days, the new process can be completed within 1 day. Importantly, this novel technique is both recyclable and scalable, making it highly suitable for industrial production. Additionally, crystallization efficiency and product yield are significantly improved. Numerous studies have highlighted the distinct bioactivity of L-gossypol [14]. In this study, multiple tumor cell lines were selected, and the cytotoxicity of the prepared L-gossypol was evaluated through a CCK-8 assay to ensure that the preparation process did not compromise its biological activity. The IC<sub>50</sub> values of L-gossypol in the tested tumor cell lines generally fall below or equal to 10  $\mu\text{mol/l}$ , notably about half of the IC<sub>50</sub> values of racemic gossypol. It is worth noting that L-gossypol (AT101) has entered phase II clinical trials as an antitumor drug. Our method has the important industrial production potential for clinical application.

## MATERIALS AND METHODS

### Materials

Gossypol acetate and threo(-)-1-(p-nitrophenyl)-1,3-dihydroxypropylamine were procured from Aladdin

Biotechnology Co., Ltd. (Shanghai, China), while the Gossypol acetate standard sample was sourced from Sigma Co., Ltd. (Michigan, USA). All chemicals, including petroleum ether, sodium bicarbonate, glacial acetic acid, acetone, ether, n-hexane, chloroform, ethyl acetate, anhydrous sodium sulfate, chromatography silica gel G, and d-DMSO, were of analytical grade and obtained from Sinopharm Group (Shanghai, China). The CCK-8 kit used in the study was purchased from Beyotime Biotechnology Co., Ltd. (Shanghai, China). Human cancer cell lines MCF-7, A549, PC-3, and BEL-7402 were acquired from ATCC.

### Methods

#### Separation of L-gossypol by improved column chromatography

Initially, an improved column chromatography method was employed to isolate L-gossypol, yielding high-purity L-gossypol samples and seed crystals. The process of preparing L-gossypol via the column separation method involves 3 key steps: the derivatization reaction of racemic gossypol, chromatographic separation of racemic gossypol derivatives, and the removal of the resolving agent. In a flask, 1.2 g of gossypol and 1.12 g of the resolving agent, threo(-)-1-(p-nitrophenyl)-1,3-dihydroxypropylamine, were dissolved in 50 ml of acetone. The solution underwent stirring and reflux at 60 °C using a collector-type constant temperature heating magnetic stirrer (DF-101S type, Changcheng Co., Ltd., Zhengzhou, China). A thin-layer chromatography (TLC) was employed to monitor and assess the binding effect. After 1 h, the reaction was deemed complete, resulting in the solution of racemic gossypol derivatives. The purification and separation of L-gossypol-resolving agent derivatives were accomplished using a silica gel column and an automatic liquid chromatography separator (QT-8B type, Shanghai Qite Analytical Instrument Co., Ltd., Shanghai, China). Subsequently, the solution of L-gossypol derivatives was concentrated, dried, and analyzed by TLC. For further processing, 100 mg of the derivative was dissolved in 20 ml of ether, followed by the addition of 2 ml of glacial acetic acid, 1 ml of concentrated hydrochloric acid, and a small amount of ascorbic acid. The mixture was stirred and refluxed at 39 °C for 4 h. After completion, an ether-acid water layer was obtained, allowing the recollection of threo(-)-1-(p-nitrophenyl)-1,3-dihydroxypropylamine from the acid water layer. The ether layer underwent washing with pure water and 1% NaHCO<sub>3</sub> until neutral, followed by an additional wash with an equal volume of pure water. To remove residual water from the ether solution, a small amount of anhydrous Na<sub>2</sub>SO<sub>4</sub> was added, and the solution was then filtered. Finally, the anhydrous ether phase was treated with a small amount of glacial acetic acid and subjected to an ultrasonic cleaning machine (KQ3200DE, Kunshan Ultrasonic Instrument

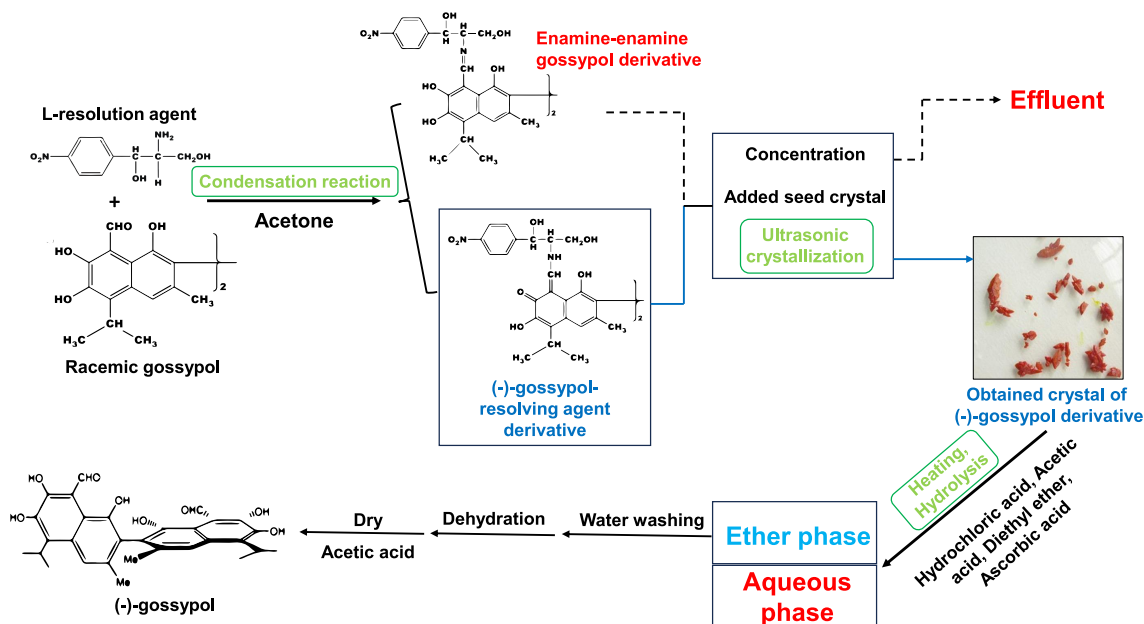


Fig. 1 The main process of the novel method developed in this study for separating L-gossypol.

Factory, China) for 3 min to obtain L-gossypol acetate crystals.

To validate the effective separation of the L-gossypol-resolving agent derivative and L-gossypol, the two products obtained from column separation were individually dissolved in acetone solutions. Subsequently, they were subjected to a digital automatic polarimeter (WZZ-2S, Jingke Instrument Co., Ltd., Shanghai, China) with a wavelength of 589 nm to measure their specific optical rotation. The mass of the products was meticulously weighed using an electronic analytical balance to calculate the yield.

$$[\alpha]_{\lambda}^t = \frac{\alpha}{C \times L} \quad (1)$$

The temperature at the time of measurement is generally 20 °C,  $\lambda$  is the wavelength of the light source used (589 nm, marked as D),  $\alpha$  is the measured optical rotation (°),  $C$  is the concentration of the solution (g/ml), and  $L$  is the length of the liquid tube (dm). If the total optical rotation  $\alpha$  of the mixture and the specific optical rotations  $[\alpha_1]$  and  $[\alpha_2]$  of each component are known, the mole fractions  $x_1$  and  $x_2$  of each component can be calculated by the equation:

$$\begin{cases} x_1 + x_2 = 1, \\ k \times l \times x_1 \times [\alpha_1] + k \times l \times x_2 \times [\alpha_2] = \alpha, \end{cases} \quad (2)$$

where  $l$  is the optical path length (cm) and  $k$  is the conversion factor related to the unit.

$$\text{Yield rate} = \frac{\text{L-gossypol (g)}}{\text{total gossypol (g)}} \times 100\% \quad (3)$$

To elucidate the structure of the product L-gossypol, we conducted a comprehensive analysis using UV-Vis spectrum scanning (Ultrospec 2100 pro, Biochrom, USA), Fourier Transform Infrared Spectroscopy (FTIR) (EQUINX55, Bruker, Germany), and NMR spectrum analysis (AVANCF 300 MHz, Bruker, Switzerland).

### Separation of L-gossypol by ultrasonic crystallization

As shown in Fig. 1, the crystallization-based preparation of L-gossypol involves 3 stages: synthesis of the racemic gossypol-resolving agent derivative, ultrasonic-induced crystallization of the L-gossypol-resolving agent derivative, and subsequent hydrolysis and purification of L-gossypol. Initially, racemic gossypol-resolving agent derivative and seed crystals of L-gossypol-resolving agent derivatives were obtained following the previously outlined method. The racemic gossypol derivative powder was dissolved in 4 solvents (acetone, methanol, ethyl acetate, and diethyl ether) to create solutions of varying concentrations. Each solution received a small amount of seed crystals and underwent ultrasonic treatment in an ultrasonic cleaner with a frequency of 40 kHz. The solutions were then refrigerated for low-temperature crystallization, yielding crystals of the L-gossypol-resolving agent derivative. Following 3 washes with petroleum ether, the crystals were dried. Parameters such as ultrasonic time, crystallization temperature, mixed solution concentration, and ultrasonic duration were systematically explored. Subsequently, the obtained solid of L-gossypol-resolving agent derivative under-

went the removal of the resolving agent, as detailed earlier, resulting in L-gossypol crystals. The L-gossypol obtained through ultrasonic crystallization underwent physicochemical analysis, the crystal yield and overall yield were calculated using relevant formulas. The bioactivity of L-gossypol obtained through ultrasonic crystallization was assessed using the CCK-8 method. Tumor cell lines MCF-7, A549, PC-3, and BEL-7402 were employed to evaluate the cell inhibitory activity of L-gossypol.

## RESULTS

### Separation of L-gossypol by improved column chromatography

Column chromatography serves as a fundamental technique for the separation and preparation of various compounds. In this study, modifications were introduced to enhance the traditional column chromatography method for isolating L-gossypol. The TLC results reveal a lack of tailing or smearing spots at each step, indicating complete reactions and the successful attainment of pure target compounds. The overall reaction process can be considered as approaching the ideal. The physical and chemical test results presented in Table 1 indicate that the specific optical rotations of L-gossypol-resolving agent derivatives and L-gossypol closely align with those reported by Si et al [15]. Additionally, considering the reported specific optical rotations of  $+357^\circ$  for D-gossypol and  $-354^\circ$  for L-gossypol, we employed these values in a calculation formula. The optical purity of the final product was determined to be 98.60%, highlighting a relatively high level of optical purity achieved by this process. The yield of L-gossypol through the column chromatography separation method reached 30.20%.

From Fig. 2(a–c), it is evident that the UV-Vis spectrum undergoes significant changes during the resolution of racemic gossypol, indicating a series of chemical transformations during the process and the generation of different intermediate products. However, the UV-Vis spectra of L-gossypol-resolving agent derivatives (Fig. 2b) and D-gossypol derivatives (Fig. 2c) exhibit remarkable similarity, suggesting that the two may share the same chemical structure (except for different configurations). This not only enhances efficiency but also yields crucial crystal seeds of L-gossypol-resolving agent derivatives. Fig. 2d and 2e show case the  $^1\text{H-NMR}$  detection spectra and photograph of the L-gossypol-resolving agent derivative. The detection results align with the target compound, and the  $^1\text{H-NMR}$  peaks of the L-gossypol-resolving agent derivative are detailed in Table S1. Analysis of the  $^1\text{H-NMR}$  spectrum reveals distinct characteristic peaks for both threo(-)-1-(p-nitrophenyl)-1,3-dihydroxypropylamine and gossypol. For gossypol, signals at 1.40 and 1.85 ppm correspond to methyl groups (positions 12, 13, and 14), 3.18 and 3.37 ppm to protons near hydroxyl groups,

**Table 1** Comparison of the specific optical rotations of L-gossypol-resolving agent derivative samples and L-gossypol samples between this study and that of Zheng et al [24].

Sample	L-gossypol-resolving agent derivative	L-gossypol
Specific optical rotation (Calculated value)	$-960^\circ$	$-344^\circ$
Specific optical rotation (Literature value)	$-968^\circ$	$-354^\circ$

6.26, 6.73, and 6.83 ppm to aromatic protons, and 13.48 ppm to phenolic hydroxyls. For the resolving agent, peaks at 3.81, 4.01, and 5.13 ppm represent the  $-\text{NCH}_2$ ,  $\text{CHOH}$ , and  $\text{CH-Ar-NO}_2$  groups, respectively, while 7.63 and 8.22 ppm correspond to aromatic protons of the nitrophenyl ring. The L-gossypol-resolving agent derivative underwent hydrolysis under acidic conditions to obtain L-gossypol samples, which exhibited high purity through comparison with standard samples and analysis via FTIR and  $^1\text{H-NMR}$  detection. As illustrated in Fig. 3b, both the L-gossypol standard and the sample exhibit identical UV-Vis absorption characteristics, with maximum absorption peaks at 364 nm and 365 nm, respectively.

The 1 nm difference between the sample and the standard peaks confirms that the final product of the racemic gossypol was L-gossypol. Fig. 3c displays the infrared absorption spectrum of L-gossypol, and the assignment of the infrared absorption peaks is analyzed (Table S2). This FTIR spectrum exhibits characteristic vibrational peaks of typical functional groups in the structure of L-gossypol, including phenolic hydroxyls ( $1285$ ,  $1379$ ,  $3419\text{ cm}^{-1}$ ), aldehyde groups ( $1616$ ,  $2610\text{ cm}^{-1}$ ), aromatic rings ( $1611$ ,  $1506\text{ cm}^{-1}$ ), and isopropyl groups ( $1177\text{ cm}^{-1}$ ). In particular, the multiple signals in the O–H and C=O regions provide strong evidence for structural confirmation and functional group analysis. Additionally, Fig. 3d presents the NMR hydrogen spectrum of L-gossypol, with the assignment of the peaks analyzed (Table S3). This  $^1\text{H-NMR}$  spectrum clearly displays multiple characteristic peaks of L-gossypol, notably the significant downfield shifts of phenolic hydroxyl groups (6.44 ppm and 15.22 ppm) and aldehyde protons (11.15 ppm). The mid-to-low field signals from isopropyl and aromatic protons further support structural confirmation. These distinct peaks serve as key indicators for verifying the structure and assessing the purity of L-gossypol.

### Separation of L-gossypol by ultrasonic crystallization

While this study has made improvements to the column chromatography separation of L-gossypol, the process remains time-consuming and labor-intensive, posing challenges for efficient high-yield production of L-gossypol. Consequently, a new process based on ultrasound-assisted crystallization was developed,

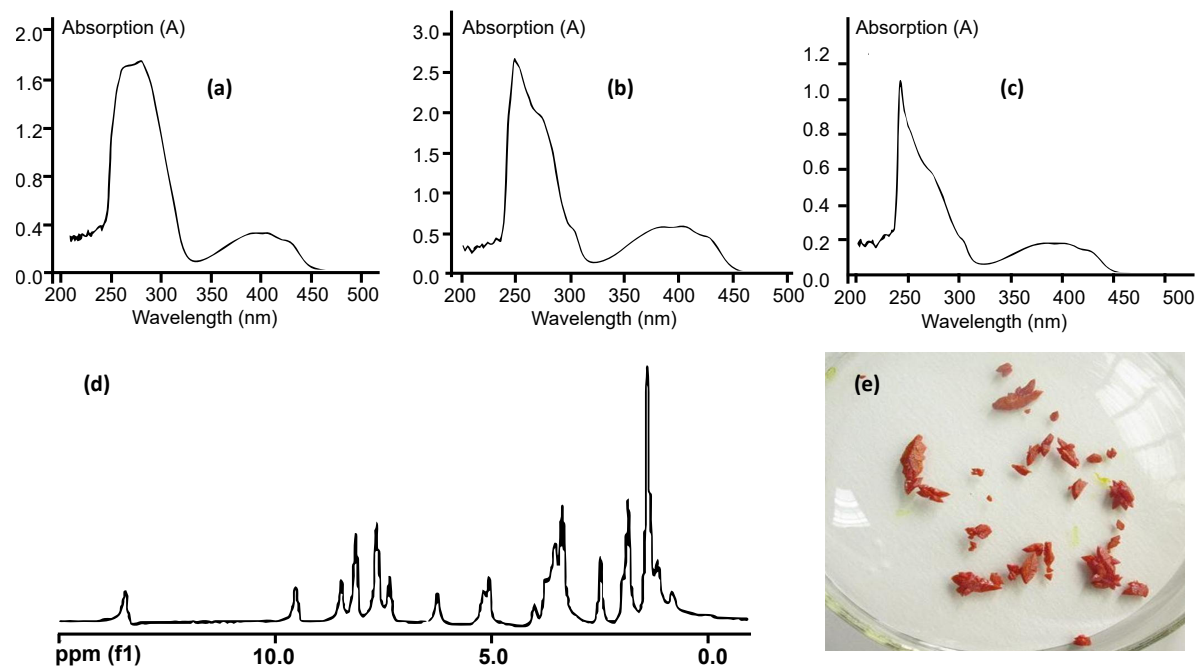


**Fig. 2** The UV-Vis absorption spectrum of racemic gossypol-resolution agent derivatives (a), L-gossypol-resolving agent derivative (b), and D-gossypol-resolving agent derivative (c). The  $^1\text{H}$ -NMR spectrum of L-gossypol-resolving agent derivative (d). Photograph of crystal of L-gossypol-resolving agent derivative (e).

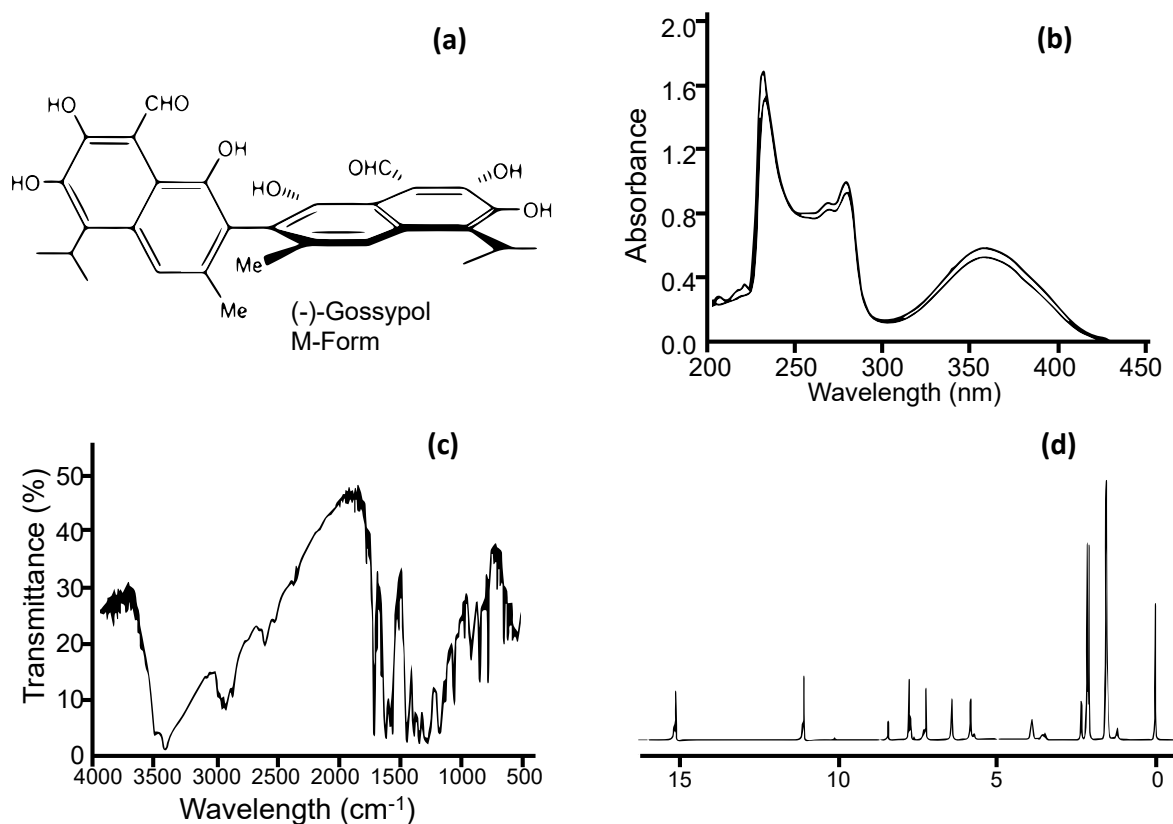


**Fig. 3** The space molecular structure of L-gossypol (a), The UV-vis absorption spectra of L-gossypol product and standard samples (b), The infrared absorption spectrum of L-gossypol (c), and The  $^1\text{H}$ -NMR spectrum of L-gossypol (d).

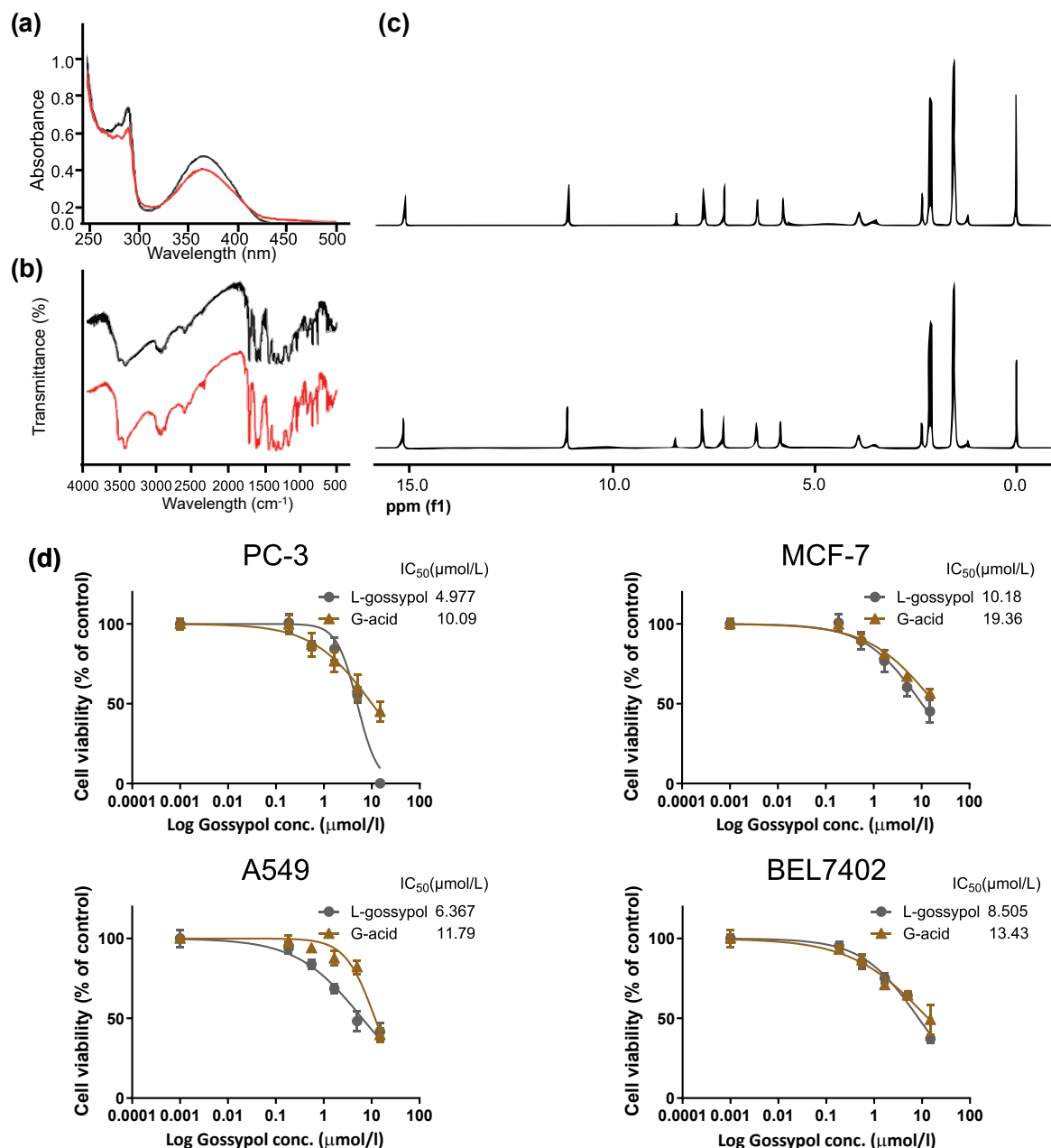


**Fig. 4** UV-Vis absorption spectra of L-gossypol product and standard samples (a), Infrared absorption spectra of L-gossypol product and standard samples (b), <sup>1</sup>H-NMR spectra of L-gossypol product and standard samples (c), and The anti-proliferation effect of L-gossypol and racemic gossypol on tumor cells (d).

resulting in the successful obtainment of L-gossypol. Ultrasound-assisted crystallization focused on separating and obtaining the L-gossypol-resolving agent derivative. Within 24 h of ultrasonic crystallization, rhombohedral crystals or crystal aggregates with a length of 0.5–1 cm were produced, achieving a crystal yield of 43.80% and optical purity of 97.89%. After hydrolysis, the total yield reached 40.45%, with an optical purity of 97.07%. UV-Vis absorption spec-

tra analysis of the L-gossypol product and standard samples (Fig. 4a) revealed identical UV-Vis absorption characteristics, with maximum absorption peaks at 364 and 364.5 nm, respectively.

The 0.5 nm difference confirmed that the final product obtained by the experimental resolution of racemic gossypol was L-gossypol. Fig. 4b illustrates the infrared absorption spectra of L-gossypol samples obtained through the new separation method and



standard samples of L-gossypol, both exhibiting high degree of consistency. The analysis results showcase infrared absorption peaks of the samples (Table S4). <sup>1</sup>H-NMR detection spectra of the L-gossypol product sample and L-gossypol standard sample (Fig. 4c) align with the target compound. The <sup>1</sup>H-NMR peaks of L-gossypol samples are detailed in Table S5. To further visually demonstrate the advantages of the craft developed in this study, a comparison was made with relevant reports on the chiral separation method of L-gossypol. The primary aspects considered in the comparison included purity, yield, production output, production duration, and cost, fully reflecting the excellent industrial potential of the process developed in this study. The details are presented in Table S6.

### Bioactivity of L-gossypol sample

It is crucial to ascertain whether the L-gossypol prepared using the new process effectively retains its expected biological activity. To assess this, a CCK-8 assay was conducted on 4 types of tumor cell lines: PC-3, MCF-7, A549, and BEL7402. The results demonstrated strong inhibitory effects in a concentration-dependent manner (Fig. 4d). Calculated by linear regression, when cells were cultured for 72 h, the IC<sub>50</sub> values of L-gossypol in the 4 tumor cell lines were 4.977, 10.18, 6.367, and 8.505 μmol/l, respectively. In comparison, the IC<sub>50</sub> values of racemic gossypol were 10.09, 19.36, 11.79, and 13.43 μmol/l, respectively. The comparison revealed that the same dose of L-gossypol had a stronger inhibitory effect on tumor cells, and the sensitivity of cells to L-gossypol was higher than that to racemic gossypol. This result underscores that the L-gossypol prepared by this process retains higher anti-cell proliferation activity.

### DISCUSSION

Gossypol, as a natural component with significant economic value, holds extensive potential for applications across diverse fields [18–21]. However, being an enantiomeric substance, separation of enantiomers is important [22, 23] and it was found that the primary biological activity of gossypol is associated with the levorotatory conformation [24, 25]. Chiral separation of gossypol poses a challenging problem. Currently, L-gossypol is predominantly obtained through an indirect method, involving the reaction of a resolving agent with racemic gossypol to produce gossypol derivatives with significant differences in physical properties. Subsequent column chromatography is then employed for separation. However, these preparation processes are characterized by complexity, time-intensiveness, high costs, and low yields [16, 17]. While Dowd [12] improved the preparation process of L-gossypol using the acetone solution crystallization method, the entire process still spans several days. The reported chiral

separation methods of gossypol outlined above have various shortcomings, primarily limited to laboratory research. These methods face challenges when scaling up for large-scale industrialization.

This study initially improved upon traditional column chromatography, achieving a final product optical purity of 98.60% with a yield of 30.20%. However, this method heavily relies on column chromatography separation, taking over 3 days for the entire process and proving challenging to scale up further. The revelation that combining chiral resolving agents with racemic gossypol generates derivatives with significant differences inspired a shift in focus. Subsequently, we directed our efforts towards the direct separation of L-gossypol-resolving agent derivatives. Taking a progressive step, we selected the cost-effective compound threo(-)-1-p-nitrophenyl)-1, 3-dihydroxypropylamine as a resolution agent to prepare L-gossypol-resolving agent derivatives, obtaining crystals of these derivatives. We introduced the ultrasonic-enhanced crystallization method, which reduced the crystallization time by more than half, further enhancing the process. Four factors, including the choice of crystallization solvent, concentration of crystallization solution, time control of ultrasonic radiation, and temperature control of crystallization, were evaluated for their impact on the yield and purity of L-gossypol. Under optimal conditions, with a concentration of 0.3 g/ml in the ethyl acetate solution, a crystallization temperature below –20 °C, and an ultrasonic crystallization time of approximately 1 min, the crystal achieved a maximum optical purity of 97.89%. After removing the resolving agent, the total yield of L-gossypol reached 40.45%, with an optical purity of 97.07%. Compared to the preparation of L-gossypol using improved column chromatography, the ultrasonic-induced crystallization method streamlined the resolution steps, shortened the crystallization time, and reduced preparation costs. While the previously reported crafts required over 4 days [12], the new process could be completed within 1 day. Importantly, this new craft is recyclable and scalable, making it highly suitable for further industrial production. Additionally, the crystallization efficiency and product yield were improved. There were 1 and 0.5 nm differences between the UV-Vis absorption spectra of the L-gossypol product samples obtained by improved column chromatography and ultrasonic crystallization methods, respectively. The L-gossypol prepared by the ultrasonic crystallization method closely matched the standard product. Furthermore, L-gossypol and racemic gossypol separated by ultrasonic crystallization were tested for *in vitro* anti-cell proliferation activity. The results of biological activity experiments demonstrated that the obtained L-gossypol significantly inhibited the proliferation of human prostate tumor cells, PC-3 and LNCaP, showcasing that the crystallization method retained the biological activity of L-gossypol.

## CONCLUSION

In comparison to other methods for separating L-gossypol, this study has introduced a novel approach centered on chiral resolving agents and ultrasonic crystallization. The advantages of this method include its simplicity, short processing time, and high yield. The efficient cyclic performance of this craft makes it highly suitable for large-scale industrial production. As a result, it plays a significant role in advancing the applications of L-gossypol in medicine, industry, and agriculture.

## Appendix A. Supplementary data

Supplementary data associated with this article can be found at <https://dx.doi.org/10.2306/scienceasia1513-1874.2025.066>.

**Acknowledgements:** This study was financially supported in part by Natural Science Basic Research Program of Shaanxi (No. 2024JC-YBQN-0806), Shaanxi Province University Youth Innovation Team Research Project (No. 24JP169), and the Program funded by Science and Technology and Information Bureau, Weiyang district, Xi'an, Shaanxi (No. 202223). Yun Zhou and Yizuo Li have equal status in this study.

## REFERENCES

1. Alam MB, An H, Ra JS, Lim, JY, Lee SH, Yoo CY, Lee SH (2018) Gossypol from cottonseeds ameliorates glucose uptake by mimicking insulin signaling and improves glucose homeostasis in mice with streptozotocin-induced diabetes. *Oxid Med Cell Longev* **2018**, 5796102.
2. Blackstaffe L, Shelley M, Fish R (1997) Cytotoxicity of gossypol enantiomers and its quinone metabolite gossypolone in melanoma cell lines. *Melanoma Res* **7**, 364–372.
3. Connors R, Schambach F, Read J, Cameron A, Sessions RB, Vivas L, Easton A, Croft SL, et al (2005) Mapping the binding site for gossypol-like inhibitors of *Plasmodium falciparum* lactate dehydrogenase. *Mol Biochem Parasit* **142**, 137–148.
4. Cai BC, Gong L, Zhu YY, Kong LM, Ju XM, Li X, Yang XD, Zhou HY, et al (2022) Identification of gossypol acetate as an autophagy modulator with potent anti-tumor effect against cancer cells. *J Agric Food Chem* **70**, 2589–2599.
5. Lopez-Charcas O, Herrera-Carrillo Z, Montiel-Reyes LE, Gomora JC (2016) Block of recombinant T-type calcium channels by gossypol, a potential contraceptive. *Biophys J* **110**, 440a–440a.
6. Du RL, Chow HY, Chen YW, Chan PH, Daniel RA, Wong KY (2023) Gossypol acetate: A natural polyphenol derivative with antimicrobial activities against the essential cell division protein FtsZ. *Front Microbiol* **13**, 1080308.
7. Gumustas M, Ozkan SA, Chankvetadze B (2018) Analytical and preparative scale separation of enantiomers of chiral drugs by chromatography and related methods. *Curr Med Chem* **25**, 4152–4188.
8. Guo HF, Qu YF, Sun S, Zhang KL, Zhang ZC, Zhao DX, Niu HT, Liu XD, et al (2022) Antiviral effect of the cotton plant-derived gossypol against tomato yellow leaf curl virus. *J Pest Sci* **96**, 635–646.
9. Li M, Wang D, He J, Chen L, Li H (2020) Bcl-XL: A multifunctional anti-apoptotic protein. *Pharmacol Res* **151**, 104547.
10. Liu SL, Kulp SK, Sugimoto Y, Jiang JH, Chang HL, Dowd MK, Wan P, Lin YC (2002) The (-)-enantiomer of gossypol possesses higher anticancer potency than racemic gossypol in human breast cancer. *Anticancer Res* **22**, 33–38.
11. Liu W, Gong P (2012) Research progress in (-)-gossypol for anticancer. *J Mod Oncol* **7**, 384–387.
12. Dowd MK (2003) Preparation of enantiomeric gossypol by crystallization. *Chirality* **15**, 486–493.
13. Qian SZ, Wang ZG (1984) Gossypol: a potential antifertility agent for males. *Annu Rev Pharmacol* **24**, 329–360.
14. Pal D, Sahu P, Sethi G, Wallace CE, Bishayee A (2022) Gossypol and its natural derivatives: multitargeted phytochemicals as potential drug candidates for oncologic diseases. *Pharmaceutics* **14**, 2624.
15. Si YK, Zhou J, Huang L (1986) Studies on the resolution of racemic gossypol-I. Use of t (S)-1-Methylphenylethylamine ( $\pm$ ) gossypol hexaacetate as the resolving agent. *Sci Sin Chim* **8**, 850–855.
16. Razakantoanina V, Nguyen Kim PP, Jaureguiberry G (2000) Antimalarial activity of new gossypol derivatives. *Parasitol Res* **86**, 665–668.
17. Šudomová M, Hassan ST (2022) Gossypol from *Gossypium* spp. inhibits *Helicobacter pylori* clinical strains and urease enzyme activity: bioactivity and safety assessments. *Sci Pharm* **90**, 29.
18. Tien VD, Vu VV, Vu TK (2019) A new synthetic route for preparation of enantiomers of gossypol and apogossypol from racemic gossypol. *Asian J Chem* **31**, 105–108.
19. Venkatesan T, Pillai SS (2012) Antidiabetic activity of gossypin, a pentahydroxyflavone glucoside, in streptozotocin-induced experimental diabetes in rats. *J Diabetes* **4**, 41–46.
20. Wang WJ, Li WK, Wen ZY, Wang C, Liu WL, Zhang YF, Liu JC, Ding TZ, et al (2022) Gossypol broadly inhibits coronaviruses by targeting RNA-dependent RNA polymerases. *Adv Sci* **9**, 2203499.
21. Wang X, Howell CP, Chen F, Yin JJ, Jiang YM (2009) Gossypol: a polyphenolic compound from cotton plant. *Adv Food Nutr Res* **58**, 215–263.
22. Yang CM, Tang H, Gu CZ, Han B, Jing WJ (2006) Resolution of the optical active derivatives of gossypol and the determination of its configuration. *Shandong Med J* **46**, 1–2.
23. Yang WH, Xiang SK (1995) The separation of gossypol enantiomers by  $\mu$ Bondapak C18 column. *Chin J Chromatogr* **13**, 264–266.
24. Zheng DK, Meng J, Si Y, Ma S, Huang L (1990) Studies on the resolution of racemic gossypol. IV. Use of threo (-) or (+)-1-(p-nitrophenyl)-1,3-dihydroxypropylamine-2 as the resolving agent. *Acta Pharm Sin* **25**, 430–434.
25. Zheng DK, Si YK, Meng JK, Huang L (1990) Studies on the resolution of racemic gossypol. II. By chiral alpha-methylphenethylamine and alpha-methylbenzylamine. *Acta Pharm Sin* **25**, 417–422.



## Appendix A. Supplementary data

**Table S1** NMR peak data for L-gossypol-resolving agent derivatives.

<sup>1</sup> H-NMR (ppm)			
1.40	d	12	12-CH <sub>3</sub> , 12'-CH <sub>3</sub> , 13-CH <sub>3</sub> , 13'-CH <sub>3</sub>
1.85	s	1	1C
2.48	s	6	14-CH <sub>3</sub> , 14'-CH <sub>3</sub>
3.37	m	2	11-CH, 11'-CH
3.18	m	2	1-C-OH, 1'-C-OH
3.81	m	2	-NCH-
4.01	d	4	O <sub>2</sub> N-Ar-(CHOH) <sub>2</sub> -
5.13	d	2	-CH-Ar-NO <sub>2</sub>
6.26	s	2	1-C-OH, 1'-C-OH
6.73	m	4	4-C-H, 4'-C-H
6.83	s	2	15-CH, 15'-CH
8.22,7.63	m	16	-C <sub>6</sub> H <sub>4</sub>
13.48	m	2	6-OH, 6'-OH

**Table S2** Infrared (IR) spectral data for L-gossypol obtained through improved column chromatography.

IR KBr (cm <sup>-1</sup> )		
3481	$\nu_{\text{O-H}}$	Stretching vibration of O—H bond in alcohol hydroxyl group
3419	$\nu_{\text{O-H}}$	Stretching vibration of O—H bond in phenol hydroxyl group
2610	$\nu_{\text{O=C-H}}$	Stretching vibration of aldehyde group C—H bond
1709	$\nu_{\text{C=O}}$	Stretching vibration of the C=O bond in acetic acid
1616	$\nu_{\text{C=O}}$	Stretching vibration of the C=O bond in the aldehyde group
1611, 1506	$\nu_{\text{C=C}}$	Skeletal vibration of the C=C bond in the aromatic nucleus
1578	$\nu_{\text{C=C}}$	Stretching vibration of C=C bond
1379	$\delta_{\text{C-OH}}$	Bending vibration of the O—H bond in the phenol hydroxyl group
1285	$\nu_{\text{O-H}}$	Stretching vibration of O—H bond in phenol hydroxyl group
1177	$\nu_{\text{C-C}}$	Skeletal vibration of the C—C bond in the isopropyl group

**Table S3** NMR peak data for L-gossypol obtained through improved column chromatography.

<sup>1</sup> H-NMR (ppm)			
1.53	d	12	12-CH <sub>3</sub> , 12'-CH <sub>3</sub> , 13-CH <sub>3</sub> , 13'-CH <sub>3</sub>
2.17	s	6	14-CH <sub>3</sub> , 14'-CH <sub>3</sub>
2.28	s	3	13-CH <sub>3</sub>
3.63	m	2	11-CH
5.74	s	2	1-C-OH, 1'-C-OH
6.44	s	2	6-C-OH, 6'-C-OH
7.83	s	2	4-C-H, 4'-C-H
8.44	s	1	17-COOH
11.15	s	2	15-CHO, 15'-CHO
15.22	s	2	7-C-OH, 7'-C-OH

**Table S4** IR spectral data for L-gossypol obtained through the new method.

IR KBr (cm <sup>-1</sup> )		
3484	$\nu_{\text{O-H}}$	Stretching vibration of O—H bond in alcohol hydroxyl group
3425	$\nu_{\text{O-H}}$	Stretching vibration of O—H bond in phenol hydroxyl group
2608	$\nu_{\text{O=C-H}}$	Stretching vibration of aldehyde group C—H bond
1716	$\nu_{\text{C=O}}$	Stretching vibration of the C=O bond in acetic acid
1616	$\nu_{\text{C=O}}$	Stretching vibration of the C=O bond in the aldehyde group
1583	$\nu_{\text{C=C}}$	Stretching vibration of C=C bond
1376	$\delta_{\text{C-OH}}$	Bending vibration of the O—H bond in the phenol hydroxyl group
1283	$\nu_{\text{O-H}}$	Stretching vibration of O—H bond in phenol hydroxyl group
1180	$\nu_{\text{C-C}}$	Skeletal vibration of the C—C bond in the isopropyl group

**Table S5** NMR peak data for L-gossypol obtained through the new method.

1 H-NMR (ppm)			
1.57	d	12	12-CH <sub>3</sub> , 12'-CH <sub>3</sub> , 13-CH <sub>3</sub> , 13'-CH <sub>3</sub>
2.15	s	6	14-CH <sub>3</sub> , 14'-CH <sub>3</sub>
2.30	s	3	13-CH <sub>3</sub>
3.61	m	2	11-CH
5.75	s	2	1-C-OH, 1'-C-OH
6.42	s	2	6-C-OH, 6'-C-OH
7.81	s	2	4-C-H, 4'-C-H
8.48	s	1	17-COOH
11.12	s	2	15-CHO, 15'-CHO
15.19	s	2	7-C-OH, 7'-C-OH

**Table S6** The relevant parameters of the main reported methods for chiral separation of L-gossypol.

Method	Optical purity (%)	Yield (%)	Output	Duration	Cost	Industrialization potential
CDR+HPLC [16]	>95	\	μg scale	≤12 h	expensive	None
CDR+Column Chromatography [15]	98.8	55.8	mg scale	>1 d	ordinary	Small
CDR+Column Chromatography [17]	≈98 (L-gossypol derivatives)	\	mg scale	>1 d	\	None
Crystallization [12]	99.6%	51.9	g scale	≥4 d	affordable	Normal
The present study	97.07%	40.45	g scale	≤1 d (recyclable)	inexpensive	Huge

\: The reference did not explicitly state this.